ISSN 1063-7834, Physics of the Solid State, 2016, Vol. 58, No. 11, pp. 2196–2202. © Pleiades Publishing, Ltd., 2016.
Original Russian Text © A.M. Klushin, E.E. Pestov, M.A. Galin, M.Yu. Levichev, 2016, published in Fizika Tverdogo Tela, 2016, Vol. 58, No. 11, pp. 2121–2126.

SUPERCONDUCTIVITY

High-Temperature Superconductor Josephson Junctions for Voltage Standards

A. M. Klushin[a], E. E. Pestov[a, b, *], M. A. Galin[a], and M. Yu. Levichev[a]

[a] *Institute for Physics of Microstructures, Russian Academy of Sciences, ul. Akademicheskaya 7, Afonino, Nizhny Novgorod oblast, 607680 Russia*

[b] *Lobachevsky State University of Nizhny Novgorod, pr. Gagarina 23, Nizhny Novgorod, 603950 Russia*

** e-mail: pestov@ipmras.ru*

Abstract—This paper presents the results of investigations of the high-frequency properties of multi-junction Josephson circuits based on high-temperature superconductors and the specific features of their use in voltage standards.

DOI: 10.1134/S1063783416110184

1. INTRODUCTION

At present, the solution of many problems in the field of the development of promising analog and digital devices for superconducting electronics has been stimulated by the use of multi-element Josephson structures. A special place among these structures has been occupied by coherently oscillating chains of Josephson junctions, which have been used both in the development of generators of the Josephson radiation and in voltage standards [1–4]. The fundamental importance of the latter application is associated with the fact that there have not been known any other physical effects which could compete in quantum metrology with the Josephson effect in the accuracy of the reproduction of voltage unit. The use of the Josephson effect in quantum metrology is based on the fact that, under the influence of an external electromagnetic field with a frequency f, the current–voltage characteristic of the Josephson junction exhibits steps of the current at voltages

$$V_n = n_f / K_J, \quad (1)$$

where $K_J = 2e/h = 483.5979$ GHz/mV is the Josephson constant and n is an integer number. The quantized voltage (1) induced at a Josephson junctions is usually small. An increase in this voltage requires that a large number of synchronously oscillating junctions should be connected in series. The most important conditions for the synchronization of arrays of Josephson junctions are as follows: (i) small spread in the values of their parameters and (ii) the presence of an electrodynamic system that ensures the effective and uniform coupling of the Josephson junctions with the external electromagnetic radiation.

Modern technologies used for producing Josephson junctions from niobium have made it possible to synchronize chains of several tens of thousands of junctions by means of an external signal. These microcircuits have served as the basis for national voltage standards in many countries, including Russia [4, 5]. However, the necessity for cooling niobium microcircuits down to the liquid-helium temperature and the corresponding high maintenance costs, as well as the limited number of firms [6, 7] producing these microcircuits, have restricted the use of the aforementioned devices in regional centers of metrology and standardization.

In this paper, we have considered the conditions for the synchronization of arrays of shunted bicrystal Josephson junctions operating at a temperature of 77 K by means of an external signal. The successful solution of this problem will lead to the creation of new voltage standards, which, in turn, will expand the range of application of these devices in quantum metrology and radio measurement technology.

2. MICROCIRCUIT OF BICRYSTAL JOSEPHSON JUNCTIONS: TECHNOLOGY AND REQUIREMENTS TO THE PARAMETERS OF THE JUNCTIONS

As was noted above, the output voltage V of the microcircuit can be increased by connecting Josephson junctions in series and passing the total bias current through them. The parameters of the Josephson junctions and the conditions providing their operation are chosen so that voltage (1) is applied to each junction and the total voltage has the form

$$V = NV_J, \quad (2)$$

where N is the number of Josephson junctions. Condition (2) imposes stringent restrictions on the spread in

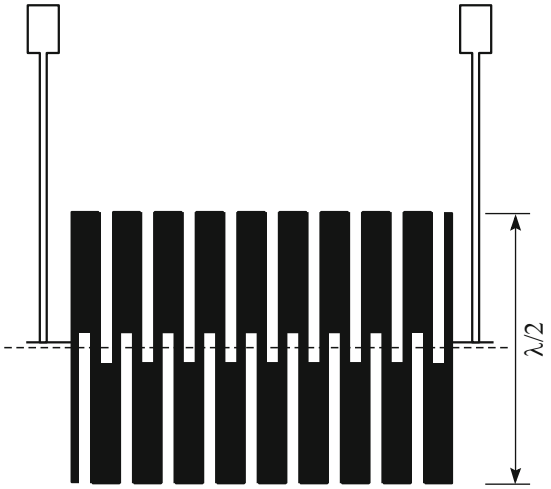

Fig. 1. Schematic representation of the topology of a chain of bicrystal Josephson junctions.

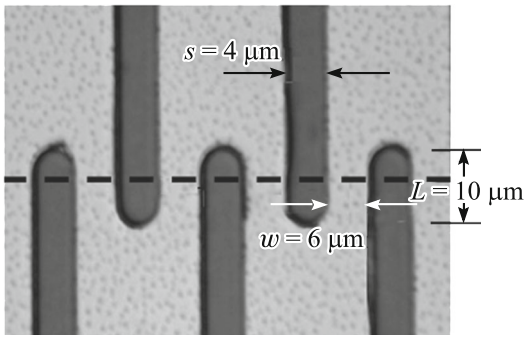

Fig. 2. Photograph of the structured high-temperature superconductor film in the form of a meander. The dashed line shows the bicrystal boundary.

the values of the parameters of the Josephson junctions and high requirements for the uniformity of their irradiation with an external signal at a frequency f. As was previously shown in [8, 9], the fulfillment of condition (2) is possible when Josephson junctions operate on the first total current step ($n = 1$) in the current–voltage characteristic if these Josephson junctions have approximately the same resistances R and the characteristic frequency $f_c \geq f$, where $f_c = K_J I_c R$ and I_c is the critical current of the junction. The conclusions drawn in [8] for niobium Josephson junctions were confirmed later in the study of chains of high-temperature superconductor Josephson junctions [10].

In the present state of the art, the only technology based on the use of bicrystal Josephson junctions has made it possible to reproducibly fabricate from them arrays on the basis of high-temperature superconductors with the required parameters. The main stages of this technology include the choice of a suitable bicrystal substrate, the growth of an epitaxial high-temperature superconductor thin film circuit on this substrate, and the circuit pattern formation using photolithography and ion etching.

For the deposition, we used bicrystal yttria-stabilized zirconia (YSZ) substrates (10 × 10 mm in size) with the misorientation angle between the crystallographic axes 2 × 12°. On each of these substrates with a size of 10 × 10 mm and a thickness of 0.5 mm, a 100- to 300-nm-thick epitaxial high-temperature superconductor $YBa_2Cu_3O_7$ (YBCO) film was grown at a temperature of 665°C and then was covered with a gold thin layer. The deposition of the two-layer structure was carried out in [11]. The gold film was deposited at a temperature of approximately 100°C in one vacuum cycle with the YBCO films, which ensured low resistivities of the junctions of the order of 10^{-8} Ω cm^2 between the two layers.

The two-layer film structure was used for the creation of arrays of shunted bicrystal Josephson junctions. Shunting was required to decrease the spread in the values of the normal resistances of the junctions, which, as already noted above, was necessary for the implementation of condition (2). The microcircuit was fabricated using standard photolithography and argon ion etching. These procedures resulted in the formation of an array of bicrystal Josephson junctions in the form of a meander, which is schematically shown in Fig. 1. A part of this array on an enlarged scale is shown in Fig. 2. It can be seen from this figure that Josephson junctions are formed at the intersection of the bicrystal boundary by the bridges. A substrate region approximately 8 mm in length contained up to 640 of such junctions.

Let us consider the effect produced by the inductance of the shunt on the current–voltage characteristics of bicrystal Josephson junctions in the framework of the resistive model [12]. In this model, three currents flow through the bicrystal Josephson junction. First, the superconducting Josephson current $I_c \sin \varphi$, where φ is the phase difference between the wave functions. Second, the current through the normal resistance of the junction R_N. Third, the current I_s through the shunt consisting of a resistor with the resistance R_s and an inductor with the inductance L_s. The system of differential equations describing the behavior of a Josephson junction in this model was solved numerically for different values of the dimensionless inductance $\beta_L = L_s/L_c$, where $L_c = \Phi_0/2\pi I_c$ is the inductance of the Josephson junction. Figure 3 shows the calculated dependences of the normalized amplitude of the first current step $\delta \equiv \Delta I_1/I_c$ on the normalized radiation frequency $\Omega = f/f_c$ for the optimum values of the microwave power. The thick solid line in Fig. 3 corresponds to the well-known case following from the resistive model for $\beta_L = 0$ [12]. With an increase in the inductance β_L (Fig. 3), the relative amplitude of the current step is slightly higher than the corresponding values of δ for $\beta_L = 0$ at low frequencies $\Omega < 0.2$.

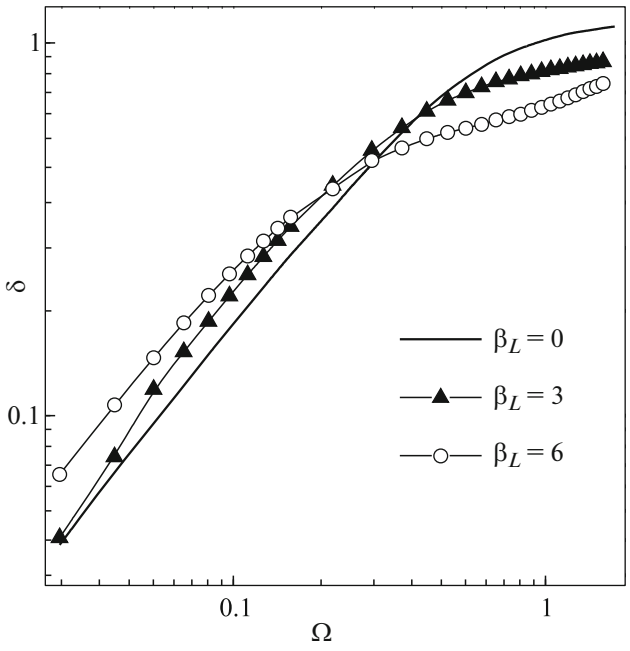

Fig. 3. Calculated dependences of the step height on the frequency.

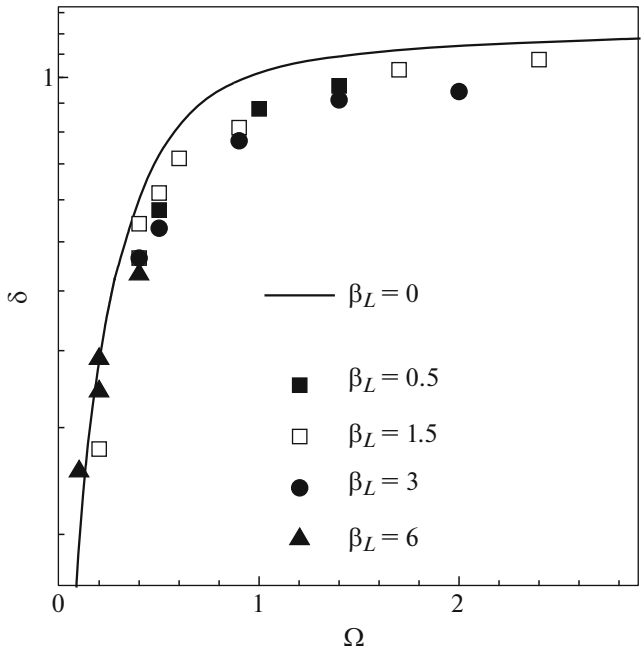

Fig. 4. Experimental (points) and calculated (solid line) dependences of the step height on the frequency.

However, at higher frequencies $\Omega > 0.3$, the relative amplitude of the current step decreases as compared to the classical case. The relative suppression of the first current step δ increases with an increase in the inductance β_L and reaches 20% for $\beta_L = 3$ and 35% for $\beta_L = 6$.

For the experimental verification of the results obtained by the numerical method, we measured the dependences of the height of the first current step δ on the frequency Ω for different values of the inductance β_L. The inductance of the shunt was changed by varying the shunt width w in the range from 3 to 18 μm and the shunt length from 20 to 4 μm. A change in the inductance of the junction L_c was also achieved by varying the critical current in the range from 0.1 to 5 mA due to the decrease of the temperature in a Dewar flask with liquid nitrogen in the range from 80 to 65 K. In contrast to the numerical simulation (Fig. 3), in the experiment, we measured only the maximum values of the amplitudes of the current steps. Therefore, these results were compared with the calculated dependence for $\beta_L = 0$ [12]. The results of the measurements are presented in Fig. 4 for the experimental values of β_L in the range from 0.5 to 6.0. For small values of the normalized frequency $\Omega < 0.2$, the step height δ follows the dependence calculated for $\beta_L = 0$ (thick solid line) even for the high inductance $\beta_L = 6$ (closed triangles). However, the deviation of the step height δ from the curve calculated for $\beta_L = 0$ increases with an increase in the frequency, Ω. For small values of $\beta_L \le 1.5$ (open and closed squares), the measured values of δ are slightly less than the calculated values for $\beta_L = 0$ in the range of frequencies Ω from 0.3 to 2.5. According to the results of the calculations presented in Fig. 4, the step height decreases by 20% for $\beta_L = 3$ (closed circles) and $\Omega = 1$.

The calculated dependences of the height of the first current step on the power of the microwave radiation are shown in Fig. 5. It can be seen from this figure that the maximum height of the current step decreases with an increase in the inductance β_L from $\delta = 1$ for $\beta_L = 0$ (thick solid line) to $\delta = 0.65$ for $\beta_L = 6$ (triangles). It is also important to note that the dependence of the amplitude of the current step on the power of the microwave radiation becomes more pronounced. This leads to the enhancement of the requirements for the uniform distribution of the microwave current along the chain of series-connected Josephson junctions, as well as the requirements for the uniformity of the distribution of the critical currents of Josephson junctions in the chain. For example, if we take the spread in the values of the critical currents of Josephson junctions in the chain to be equal to $\delta I = 2$ (see Fig. 5), the maximum value of the amplitude of the total current step decreases from $\delta = 0.8$ for $\beta_L = 0$ to $\delta = 0.5$ for $\beta_L = 6$. It is interesting to note that, with an increase in the inductance β_L, the amplitude of the current step does not decrease to zero depending on the power, as is typical for the case of $\beta_L = 0$. This specific feature was also observed experimentally.

The results presented in Figs. 3–5 indicate that the Josephson junctions are effectively shunted both by the direct current (dc) and alternating current (ac)

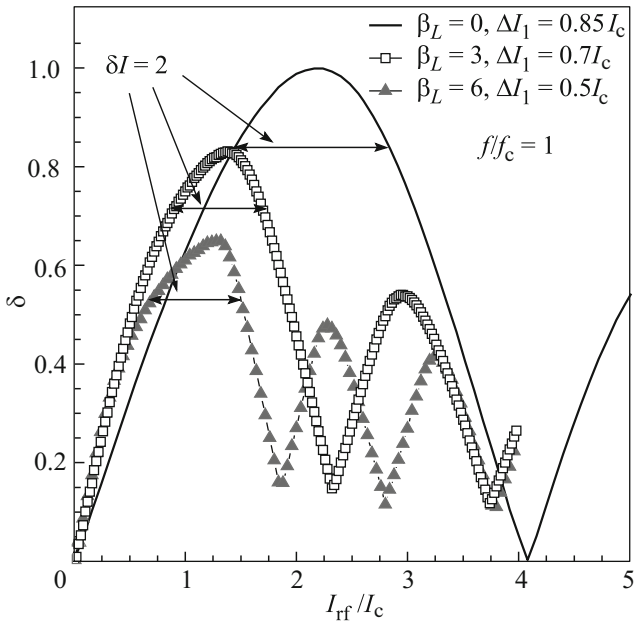

Fig. 5. Dependences of the height of the current step on the power of the microwave radiation.

only at low frequencies $\Omega \le 0.2$. At these frequencies, the impedance of the Josephson junction is predominantly determined by the active part of the resistance $R_s > 2\pi_f L_s$, and its behavior is well described by the resistive model for $\beta_L = 0$. At high frequencies $\Omega > 0.3$, the situation is complicated. The impedance of the shunt becomes reactive and is determined by the inductance of the shunt. In this case, the efficiency of the ac shunting decreases with an increase in the inductance β_L, because the ac impedance of the shunt becomes higher than the impedance of the Josephson junction. It should be noted that a significant suppression of the current steps with an increase in the inductance β_L is characteristic of only the junctions with a low capacitance, for example, high-temperature superconductor Josephson junctions. In shunted Josephson junctions with a high capacitance, a decrease in the amplitude of the current steps is not observed up to the large value of $\beta_L = 8$ [13, 14].

The calculations performed in this study demonstrated that a significant deviation from the resistive model begins to occur for the inductance $\beta_L = 1.5$. This condition restricts the maximum value of the critical current by the value of $I_{cmax} \approx 0.75\Phi_0/\pi L_s$. In order to evaluate the critical current $I_{c,max}$, it is necessary to determine the inductance of the shunt L_s, which depends on its geometrical dimensions. The width of the bridge should satisfy the well-known condition $w < 4\lambda_J$, where λ_J is the Josephson penetration depth, in order to remain in the limit of the point junction. The minimum length of the bicrystal bridge is predominantly determined by the accuracy of matching the bicrystal boundary with the middle of the bridge in photolithography and is usually equal to 4 μm. For the typical value of the surface inductance $L_\square = 1$ pH, we obtain $I_{cmax} \approx 0.7$ mA. This restriction, first, will make it difficult to use shunted Josephson junctions in programmable standards of Volta, the reliable operation of which requires the fulfillment of the condition $I_{cmax} > 1$ mA. Second, it can be significant if the influence of thermal noise on the slope of the current steps at liquid-nitrogen temperatures is taken into account. This restriction can be removed when using unshunted bicrystal Josephson junctions.

3. MICROWAVE PROBE FOR IRRADIATION OF ARRAYS OF BICRYSTAL JOSEPHSON JUNCTIONS

The Josephson structure was placed in a measurement probe immersed in a liquid nitrogen dewar. The probe is based on a circular waveguide with the length $l = 65$ cm, which, in the chosen frequency range from 70 to 76 GHz, is oversized (Fig. 6a). On each end of the waveguide, there is a transition to the WR12 standard waveguide. The end of the waveguide, which is immersed in the dewar, is connected to a round horn. After the round horn, a sample with Josephson junctions is located so that its surface is oriented parallel to the plane of the horn aperture. Behind the sample, a metallic mirror can also be placed, which makes it possible to improve the matching between the external radiation and the Josephson structure. The probe design allows one to change the relative position of the round horn, the sample, and the mirror, as well as to rotate the horn around the axis. The outside of the probe is hermetically enclosed into a metallic housing and also covered with a permalloy screen for protecting the microcircuit from external magnetic fields. Before the measurements, the housing of the probe is filled with helium, which provides the effective cooling of the microcircuit when the probe is immersed in liquid nitrogen, and also protects the sample from moisture during the heating.

The opposite end of the waveguide is connected to a source of electromagnetic radiation. It is a solid-state eight-fold multiplier, to which a signal is supplied from a frequency synthesizer in the range from 8.5 to 9.5 GHz. The multiplier cavity has the form of a rectangular waveguide section with the end wall. The fundamental mode in the cavity is excited using a pin oriented along the narrow wall of the waveguide (Fig. 6b, inset). Thus, the multiplier cavity, the circular waveguide, the round horn, and the metallic mirror form a microwave resonator. The resonator length depends on the size of gaps separating the horn, the sample, and the mirror and varies in the range from 73 to 77 cm (Fig. 6b). This resonator plays an important role in the process of matching of the Josephson junctions to the external radiation. In order to determine the influence of the frequency spectrum of the resonator, we inves-

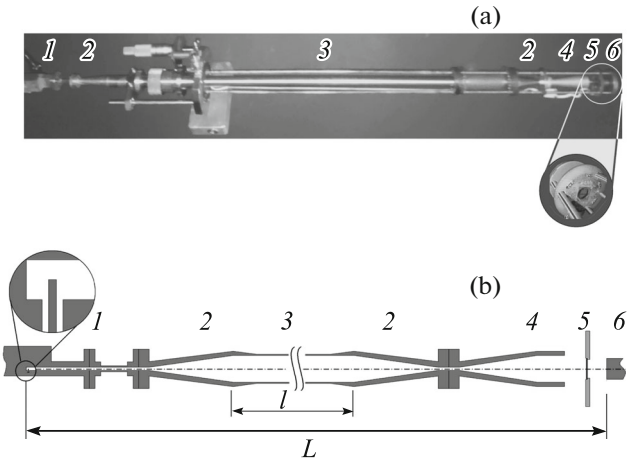

Fig. 6. (a) Exterior view and (b) schematic diagram of the measurement probe: (*1*) multiplier, (*2*) waveguide junctions, (*3*) circular waveguide, (*4*) round horn, (*5*) sample on a textolite holder, and (*6*) mirror.

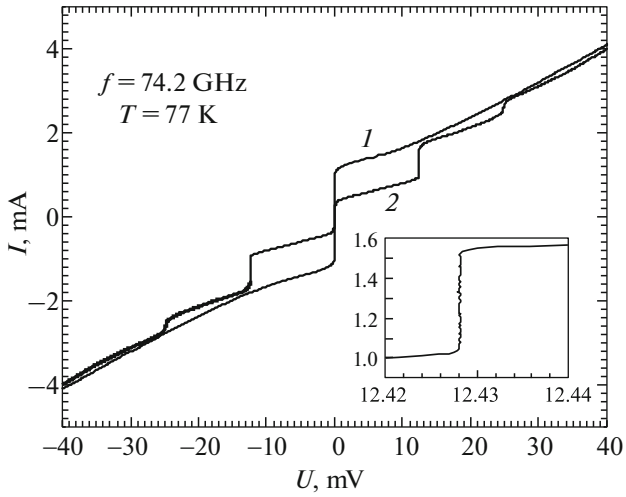

Fig. 7. Current–voltage characteristics of the microcircuit section containing 81 Josephson junctions (*1*) before irradiation and (*2*) after irradiation with a signal at a frequency $f = 74.24$ GHz. The inset shows, on an enlarged scale, the current step at a voltage of 12.428 mV.

tigated the dependence of the amplitude of the critical current on the frequency of the external signal in the range from 73 to 75 GHz. Significant suppression of the critical current was observed at several frequencies, the interval between which was approximately equal to $\Delta f = 200$ MHz. These oscillations are determined precisely by the aforementioned microwave resonator, because the effective length $c/2\Delta f = 75$ cm (where c is the speed of light) coincides up to 2–3% with the distance between the end wall of the multiplier and the matching mirror. The changes of the wave number in the circular and rectangular waveguides for these estimates were of no importance and, hence, were not considered, because the transverse wave number of the fundamental mode of the circular waveguide is significantly smaller than the wave number in the medium, and the length of the rectangular waveguide sections is short compared to the total length of the resonator. Usually, only at one of the frequencies, we observed the current steps with the maximum amplitude. Based on the above data, we can assume that, only at this frequency, the mode corresponding to the uniform distribution of the electromagnetic field over the sample surface is excited.

4. RESULTS OF THE INVESTIGATION OF ARRAYS OF BICRYSTAL JOSEPHSON JUNCTIONS

Using the results of the analysis performed in this study, we developed a circuit consisting of 640 bicrystal Josephson junctions. The circuit was fabricated on the YSZ substrate. The thickness of the YBCO film was equal to 150 nm, and the thickness of the gold film was 30 nm. The topology of chains consisting of bicrystal Josephson junctions (Figs. 1 and 2) was designed taking into account the optimization of the coupling of the array of Josephson junctions with the external electromagnetic field. For this purpose, the size of the meander in the direction perpendicular to the electric field vector was chosen to be equal to $\lambda_{eff}/2 = 0.48$ mm, where λ_{eff} is the effective wavelength in the substrate with the dielectric constant $\varepsilon = 26$. Thus, each of the meander strips forms a half-wavelength resonator at a frequency of the order 75 GHz with the maximum current in the region of the Josephson junction [15].

The current–voltage characteristics of two microcircuit sections including 80 and 81 Josephson junctions and operating at the boiling temperature of liquid nitrogen are shown in Figs. 7 and 8, respectively. For both samples, the average critical current was equal to $I_c = 0.9$ mA, and the average resistance of the shunted Josephson junctions was $R = 0.14$ Ω. The characteristic voltage of the junctions $V_c = I_c R = 126$ μV was optimum to obtain the total current steps upon irradiation at a frequency close to 75 GHz.

In the current–voltage characteristics of the arrays of 80 and 81 Josephson junctions subjected to an external signal at a frequency $f = 74.2$ GHz, the total current steps are observed at voltages of 12.275 and 12.428 mV, respectively. In the case of the microcircuit sections connected in parallel, the differential voltage at the output of the microcircuit is $\Delta V_J \cong 153$ μV, which can be used for the precise measurement of the step steepness. The measurements with a resolution of approximately 1 nV showed that, in the current–voltage characteristics of both sections, the amplitude of the current steps is approximately equal to 100 μA. In the case where these sections are connected in series, the total quantum output voltage $V_J \cong 25$ mV can be

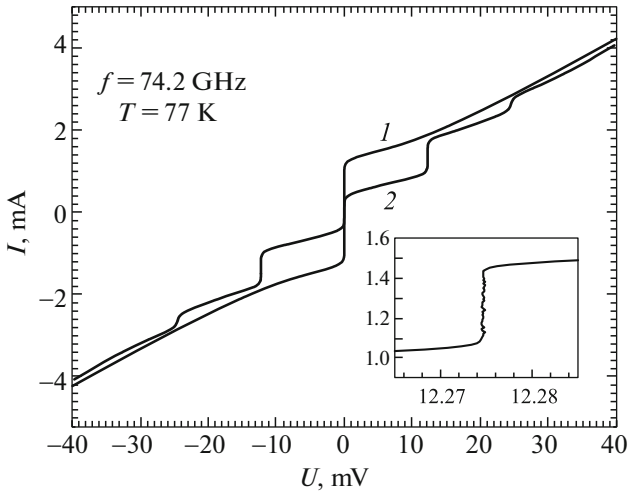

Fig. 8. Current–voltage characteristics of the microcircuit section containing 80 Josephson junctions (*1*) before irradiation and (*2*) after irradiation with a signal at a frequency $f = 74.20$ GHz. The inset shows, on an enlarged scale, the current step at a voltage of 12.275 mV.

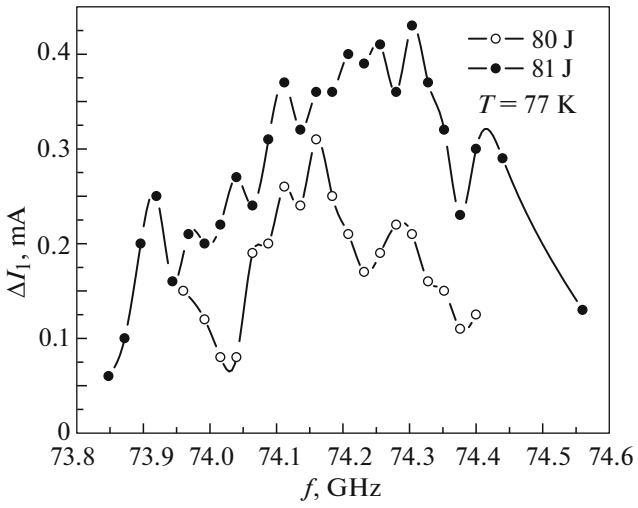

Fig. 9. Dependences of the amplitude of the current steps on the radiation frequency.

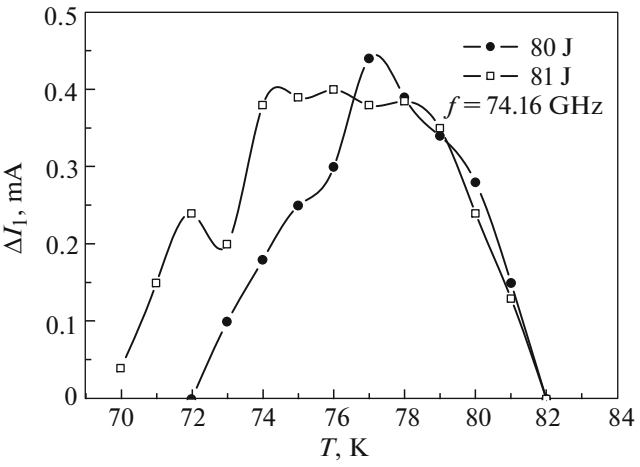

Fig. 10. Dependences of the amplitude of the current steps on the temperature.

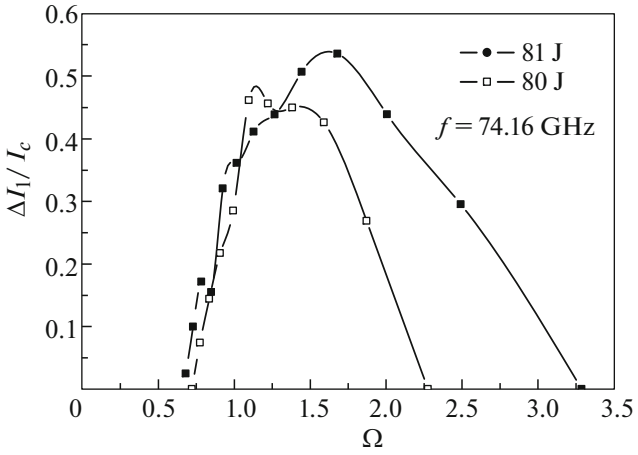

Fig. 11. Dependences of the amplitude of the current steps on the normalized radiation frequency.

used in voltage standards for the calibration of resistive dividers [16].

We also investigated the dependences of the amplitude of the total current steps on the frequency (Fig. 9) and temperature (Fig. 10). Figure 9 demonstrates a strong frequency dependence of the height of the current steps, which complicates the matching of the chain of junctions with the external radiation. Simultaneously, the current steps with an amplitude of more than 300 μA are observed in the frequency range of no more than 100 MHz. On the other hand, the temperature dependence is weaker, and in the temperature range of approximately 1 K, there are current steps with a large amplitude.

Figure 11 shows the dependences of the amplitude of the current steps on the normalized radiation frequency Ω, which confirms the conclusions previously drawn in [8]. The maximum amplitude of the current steps is observed at a frequency $\Omega = 1–2$. In order to synchronize the Josephson junctions by means of the external signal at frequencies $\Omega < 1$, it needs to operate with a smaller spread in the values of the critical currents and with a more uniform distribution over the amplitude of the microwave current in the array as compared to those achieved in our case. On the other hand, at high frequencies Ω, the amplitude of the current steps decreases due to the lack of the microwave power at the sample, because the amplitude of the desired power increases proportionally with Ω^2 [9].

5. CONCLUSIONS

In this study, we analyzed the requirements imposed on Josephson junctions, which must be satisfied to synchronize large arrays of the junctions. Despite the inevitable spread in the values of critical currents δI_c and normal resistances δR, the synchronization is possible for the normalized characteristic frequencies $\Omega \geq 1$ and small values of δR. However, strong shunting of the Josephson junctions results in the restriction of the maximum critical current, which hampers the use of the junctions at liquid-nitrogen temperatures. The use of shunted Josephson junctions with high critical currents leads to an increase in the differences between the current–voltage characteristics of the junctions as compared to the resistive model. More precisely, the amplitudes of the current steps in the current–voltage characteristics decrease. Furthermore, the requirements for the uniform distribution of the microwave current are enhanced. These features make it difficult to synchronize large arrays of Josephson junctions as well as to obtain the total current steps with large amplitudes. The analysis performed in this study demonstrated that there is a very narrow range of parameters of the Josephson junctions with the very stringent requirements imposed on the uniformity of the distribution of the microwave current, the fulfillment of which makes it possible to synchronize the Josephson junctions and to observe the total current steps. Using two microcircuit sections connected in series, we obtained the current steps at voltages of ~25 mV, which are used in voltage standards with a nitrogen cooling level of the Josephson junctions [16].

ACKNOWLEDGMENTS

The authors would like to thank V.A. Markelov, A.I. El'kina, and N.V. Rogozhkina for their assistance in performing the experiments.

This study was supported in part by the Russian Foundation for Basic Research (project nos. 15-02-05793, 15-42-02469, and 16-32-00686) and the Russian Science Foundation (project no. 15-12-10020).

REFERENCES

1. G. Wang, Z. Zhang, Y. Lu, J. Xu, and K. Zhou, Meas. Sci. Technol. **27**, 015003 (2016).
2. J. Lee, R. Behr, L. Palafox, A. Katkov, M. Schubert, M. Starkloff, and A. C. Böck, Metrologia **50**, 612 (2013).
3. T. M. Benseman, A. E. Koshelev, W.-K. Kwok, U. Welp, K. Kadowaki, J. R. Cooper, and G. Balakrishnan, Supercond. Sci. Technol. **26**, 085016 (2013).
4. J. Kohlmann, in *Applied Superconductivity: Handbook on Devices and Applications*, Ed. by P. Seidel (Wiley, New York, 2015), pp. 807–827.
5. V. S. Aleksandrov, A. S. Katkov, and A. S. Telitchenko, Izmer. Tekh., No. 3, 6 (2002).
6. Hyprs Inc. http://www.hypres.com/.
7. Supracon AG. http://www.supracon.com/.
8. S. I. Borovitskii, A. M. Klushin, T. B. Korotina, A. E. Pariiskii, S. K. Khorshev, and P. A. Shisharin, Sov. Tech. Phys. Lett. **11** (6), 275 (1985).
9. R. L. Kautz, J. Appl. Phys. **78** (9), 5811 (1995).
10. A. M. Klushin, W. Prusseit, E. Sodtke, S. I. Borovitskii, L. Amatuni, and H. Kohlstedt, Appl. Phys. Lett. **69** (11), 1634 (1996).
11. Ceraco GmbH. www.ceraco.de.
12. K. K. Likharev and B. T. Ul'rikh, *Systems with Josephson Junctions* (Moscow State University, Moscow, 1978) [in Russian].
13. J. Hassel, H. Seppä, L. Grönberg, and I. Suni, Rev. Sci. Technol. **74**, 3510 (2003).
14. Yu. M. Shukrinov, I. R. Rahmonov, K. V. Kulikov, and P. Seidel, Europhys. Lett. **110** (4), 47001 (2015).
15. A. M. Klushin, M. He, M. Yu. Levitchev, V. V. Kurin, and N. Klein, J. Phys.: Conf. Ser. **97**, 012268 (2008).
16. Measure of Voltage N4-21. http://www.kvarz.com/general/N4-21.html.

Translated by O. Borovik-Romanova